The 9th International Supercritical CO_2 Energy Technologies Symposium
March 2 - 5, 2026, Pittsburgh, PA
Paper #034

Extended Phase Diagram of Supercritical Carbon Dioxide and its Applications

Raad S. Haque
Doctoral Student
University of North Texas
Denton, Texas
Raad.haque@unt.edu

Laura M. Almara
Postdoctoral Researcher
Texas State University
San Marcos, Texas
lalmara@txstate.edu

Guo-Xiang Wang
Associate Professor
The University of Akron
Akron, Ohio
gwang@uakron.edu

Vish Prasad
Professor
University of North Texas
Denton, Texas
Vish.Prasad@unt.edu




ABSTRACT

Characterization of the thermophysical behavior of carbon dioxide (CO_2) and other fluids at supercritical (SC) state is critical to the scientific and technological advancements in energy devices, planetary science, and environmental systems. Here, we present a thermodynamic analysis based on the Gibbs free energy that identifies the anomalous region and extends the traditional phase diagram beyond the critical point. This analysis distinguishes supercritical fluids into three distinct pseudo phases: SC gas-like, SC liquid-like, and SC solid-like. The analysis also introduces a new "Dwij point," beyond which the fluid transitions directly from the gas to solid via SC gas-like and SC solid-like state without passing through the liquid phase. Consequently, this phase characterization defines the boundary of the liquid/SC liquid-like region. Recognizing and/or avoiding the anomalous region is important in the design of systems involving SC CO_2 or similar fluids. The implications of this work extend to SC Brayton cycle, ultra- enhanced thermal power systems, carbon storage at the ocean bottom and geological reservoirs, planetary modeling, ultra-long distance SC CO_2 transport, and so on.

INTRODUCTION

A recent thermodynamic analysis based on the Gibbs-free-energy, g, carried out by Wang et al. [1] has shown that the modified property functions - the isobaric specific-heat parameter ($c_p^* = c_p/T$), isobaric thermal expansion parameter, ($\beta^* = v\beta$), and isothermal compressibility parameter, ($\kappa^* = v\kappa$) - are better suited for characterization of the fluid from its subcritical to supercritical states than the conventional properties of c_p, β, and κ. The (P, T) loci of extrema of c_p^*, β^*, and κ^* form closed loops on the phase diagram and delineate the anomalous region. This region originates between the triple point and critical point and extends deep into the supercritical region [1]. Our work significantly extends this analysis by revealing the closed boundary of the liquid/SC liquid-like region together with a distinct supercritical solid-like (SCSL) state. Furthermore, a Dwij point (DP) is discovered, beyond which only two states — gas and solid — exist [2]. The analysis leads to major modifications in the Gibbs phase diagram, after 150 years.

THERMODYNAMIC MODEL

The Gibbs free energy model yields four fluid property functions: ζ_1, ζ_2, ζ_3, and ζ_4. Nishikawa's condition, $d^3g = 0$ at critical point (CP), requires that each of these functions vanish at CP. Consequently, the conditions $\zeta_1 = 0$, $\zeta_3 = 0$, and $\zeta_4 = 0$ map the anomalous region (Fig. 1) [1], and $\zeta_2 = 0$ map the boundary of the liquid/SC liquid-like state, the solid-like state, and the Dwij point (Fig. 2) [2].

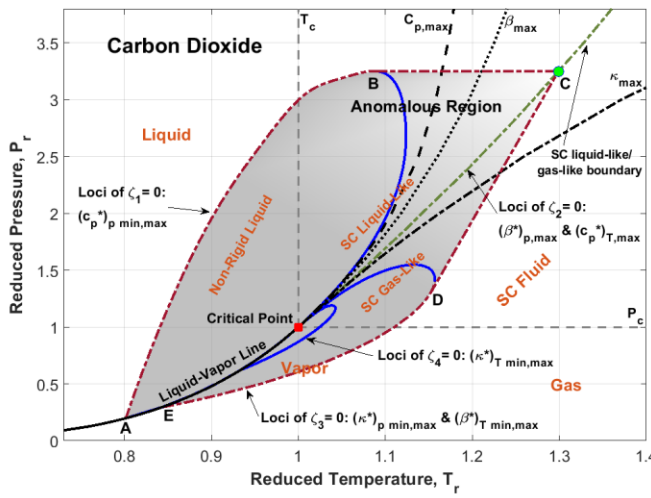

Fig. 1: Anomalous region, ABCDEA for CO_2; anomalies are maximal at CP, and they vanish outside ABCDEA

$$\zeta_1 = \left(\frac{\partial^3 g}{\partial T^3}\right)_P = -\left[\frac{\partial}{\partial T}\left(\frac{c_P}{T}\right)\right]_P = 0$$

$$\zeta_2 = \left(\frac{\partial^3 g}{\partial T^2 \partial P}\right) = \left[\frac{\partial(v\beta)}{\partial T}\right]_P = \left[\frac{\partial}{\partial T}\left(\frac{\partial v}{\partial T}\right)_P\right]_P = \left(\frac{\partial^2 v}{\partial T^2}\right)_P = 0$$

$$\zeta_3 = \left(\frac{\partial^3 g}{\partial T \partial P^2}\right) = \left[\frac{\partial(v\beta)}{\partial P}\right]_T = \left[\frac{\partial}{\partial P}\left(\frac{\partial v}{\partial T}\right)_P\right]_T = \left(\frac{\partial^2 v}{\partial T \partial P}\right) = 0$$

$$\zeta_4 = \left(\frac{\partial^3 g}{\partial P^3}\right)_T = \left(\frac{\partial(v\kappa)}{\partial P}\right)_T = -\left(\frac{\partial}{\partial P}\left(\frac{\partial v}{\partial P}\right)_T\right)_T = -\left(\frac{\partial^2 v}{\partial P^2}\right)_T = 0$$

Here, subscripts T, P denote derivatives taken along isotherms and isobars, respectively. The NIST REFPROP and WebBook are used to obtain the property data needed here, except for water, for which IAPWS-95 EOS is employed.

RESULTS AND DISCUSSION

Fig. 1 shows the anomalous region of CO_2 which is delineated by the (P, T) loci of maxima and minima of $(c_p^*)_P$, $(\kappa^*)_T$, and $(\kappa^*)_P/(\beta^*)_T$. The $\zeta_1 = 0$ loop forms a closed loop within the subcritical liquid and supercritical liquid-like regions and do not intersect the liquid–vapor line. In contrast, the loci of $\zeta_3 = 0$ and $\zeta_4 = 0$ are two distinct loops located on the right side of the liquid–vapor line, within the vapor/gas and supercritical gas-like regions. Notably, the $\zeta_4 = 0$ loop is significantly smaller, lies much closer to the critical point and is entirely enclosed by the $\zeta_3 = 0$ loop. This implies that property anomalies in the overlapping region of the $\zeta_3 = 0$ and $\zeta_4 = 0$ loci would be considerably stronger than those in the non-overlapping region. These three loops together identify the anomalous region, ABCDEA [1]. Wang et al. [1] emphasized that most supercritical systems must be operated outside the anomalous region. This is necessitated by the fact that strong variations in specific heat, density, and related properties within this region can trigger local thermodynamic non-equilibria, flow instabilities, and heat-transfer deterioration.

The SC pressure–temperature states that satisfy $\zeta_2 = 0$ are indicated by the dark green solid line in Fig. 2. The lower branch, between CP and the Dwij point (DP), represents the maxima of $(c_p^*)_T$ and $(\beta^*)_P$, whereas the upper branch, beyond DP, their minima. It starts from CP, extends deep into the supercritical region, turns at DP (P_d = 178.8 MPa, T_d = 669.1 K, ρ_d = 0.7815), and then intersects the melt-solid (S-L) line, thereby closing a loop that delineates the liquid/ SC liquid-like boundary. At DP, both the third- and fourth-order cross derivatives of g are zero:

$$\zeta_2 = \left(\frac{\partial^3 g}{\partial T^2 \partial P} \right) = 0 \text{ and } \left(\frac{\partial \zeta_2}{\partial P} \right)_T = \left(\frac{\partial^4 g}{\partial T^2 \partial P^2} \right) = 0$$

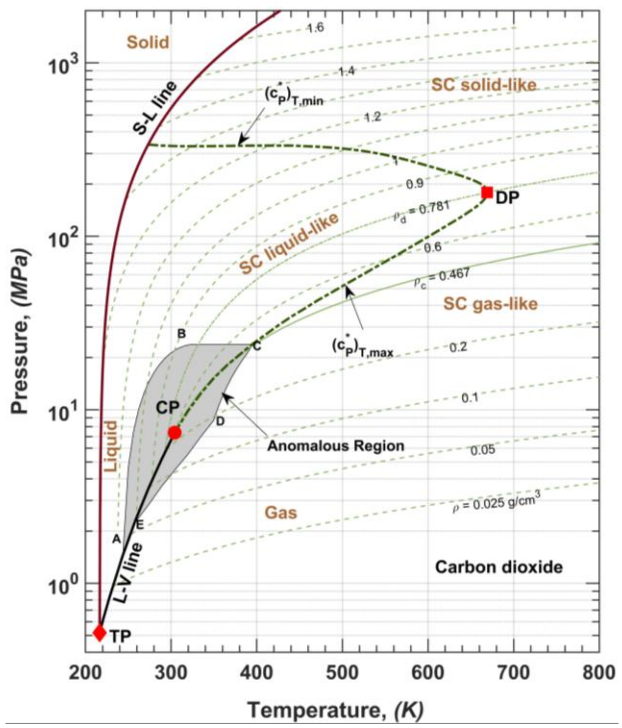

Fig. 2: Extended phase diagram for CO_2 with the anomalous region, ABCDEA and three pseudo-SC phases: gas-like, liquid-like, and solid-like; only gas and solid states exist beyond DP.

That means, $(\partial^3 v/\partial T^2 \partial P) = (\partial^2 c_p^*/\partial P^2) = (\partial^2 \beta^*/\partial T\, \partial P) = 0$ at DP. The inflection point of this curve implies that $(\partial T/\partial P) = 0$, and thus $(\partial P/\partial T)_{DP} \rightarrow \infty$, which remains finite along the liquid–vapor coexistence curve. Moreover, the lower branch of the $\zeta_2 = 0$ locus (Fig 2), which tracks the maxima of c_p^* vs P (also, β^* vs T), is the natural extension of the L-V line. This shows that, beyond the critical point and up to the Dwij point, this branch thermodynamically separates the supercritical liquid-like and gas-like states [2].

Building on the arguments for the SCLL/SCGL boundary (defined by the loci of maxima), the loci of minima (the upper part of the green line) can be interpreted as the boundary between the liquid/SC liquid-like and SC solid-like states. This hypothesis is strongly supported by the behavior of density, specific volume, isobaric thermal expansivity, and isothermal compressibility, which all show temperature effects weakening as pressure increases. Beyond DP, there exists only two phases: gas and solid. This is analogous to the region below the triple point, where only solid and vapor phases are present. The phase transition from gas to solid occurs via the SC gas-like and SC solid-like states (see [2] for more details.

Indeed, Brazhkin et al. [3] have proposed a Frenkel line (FL) to distinguish the rigid (solid-like) liquid from the non-rigid (gas-like) liquid at very high pressures and temperatures. Notably, the FL intersects the Dwij point [2]. This observation suggests that DP may represent the termination of thermodynamically dominant transitions, whereas the Frenkel line marks the onset of dynamics-dominant transitions beginning at or near DP [2].

Applications: Supercritical CO_2 (sCO_2) Brayton cycles exploit the strong variation of thermophysical properties near the critical point. This is achieved by placing the compressor inlet in the liquid-like, high-density region and the turbine inlet at much higher temperatures and pressures. As is evident from the new phase diagram (Fig. 2), the compressor is deliberately operated close to the anomalous region, whereas the expansion occurs through SC gas-like region where property variations are monotonic [4,5]. An increase in turbine inlet pressure and temperature generally leads to an improvement in cycle efficiency. In the Advanced Burner Test Reactor (ABTR) design coupled with a supercritical CO_2 recompression Brayton cycle, a net cycle efficiency of approximately 39% can be achieved at a turbine inlet temperature of about 470°C [6]. In these cycles, the main compressor inlet is maintained just above CP, placing it within the anomalous region, whereas the turbine operates at T/T_c ~ 2-3, P/P_c ~ 2-4, achieving higher cycle efficiency than conventional power cycles [4,5,6].

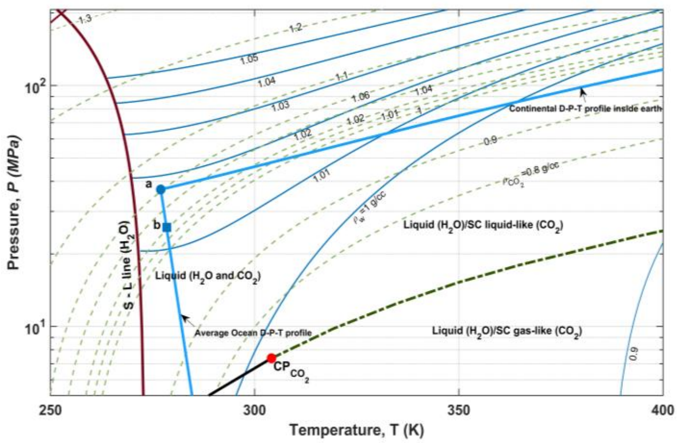

Fig. 3: Combined density contours of CO_2 (dashed green line) and H_20 (solid light-blue line). The blue line up to “a” presents the depth-pressure-temperature (*D-P-T*) profile at average ocean (“b” at 2700 m and “a” at 3700 m); further extension of this line represents the continental condition of *D-P-T.*

Carbon dioxided can be sequestrated in the ocean where the density of CO_2 would be grater than density of water. This injected CO_2 may remain isloated from the atmosphere for several hundreds of years. Studies show that CO_2 must be released below ~500 m depth; above that, the pressure is insufficient to prevent the CO_2 from transitioning to a gas phase, causing it to bubble toward the surface. Below ~500 m, CO_2 will be in a liquid form [7]. As per Fig. 3, between 500 and 2700 m depth, liquid CO_2 is still buoyant in water due to its low density and would tend to rise. Indeed, CO_2 can become denser than water only after ~2700 m depth, where the pressure is ~ 27 MPa (point “b” in Fig. 3). Thus, injecting CO_2 at mid-ocean depths would not result in stable sequestration, as the buoyant liquid CO_2 droplets would ascend, gradually dissolving and potentially reaching the surface. At greater depths (~3000 m and below), the situation would be much better (P > 30 MPa); CO_2 would be significantly denser than seawater, causing it to sink to the bottom and remain there.

For geological sequestration in subsurface formations, CO_2 is proposed to be injected as a SC fluid into the deep porous rock, such as saline aquifers or depleted oil/gas reservoirs. Depth is a critical criterion: formations deeper than about 800–1000 m are generally required so that CO_2 will be in a dense liquid/SC liquid-like state. A fascinating scenario would involve injecting CO_2 that acquires its SC solid-like state as it goes deeper, where the pressure and temperature become higher. Indeed, deep reservoirs could be a much better target, as CO_2 will transition to more stable SC solid-like state after ~8.6 km of depth. Of course, that would require a big leap in drilling technology.

As reported, for the pipeline transport of CO_2, the operating conditions need to be deliberately kept in a single, dense phase to minimize the compression work and avoid the two-phase region. This would also avoid strong anomalies that can cause large pressure drops and transient problems. Large-scale pipeline systems generally operate CO_2 under dense phase at pressures above about 8–10 MPa and temperatures between roughly 273 and 303 K to avoid two-phase flow while maintaining high compressibility efficiency and low specific volume [8]. The reality is that a part of the dense phase, above and below CP, certainly belongs to the anomalous region [9]. Indeed, in the CO_2 phase diagram (Fig. 3), this operating window lies just above the CP and within the SC liquid-like state, which is part of the anomalous region. In this region, small changes in temperatures or pressures—caused by factors like ambient elevation—may lead to instabilities. We believe, that with the availability of our new phase diagram (Fig. 3), it is possible to develop better designs for the transport of SC CO_2 that entirely avoids the anomalous region along the pipeline, as demonstrated for the supercritical natural gas transport (SNG) in [10].

REFERENCES

[1] G.-X. Wang, L.M. Almara, and V. Prasad, Thermodynamic analysis of anomalous region, critical point, and transition from subcritical to supercritical states: Application to van der Waals and five real fluids, *Phys. Fluids*, 36 (2), 2024.

[2] V. Prasad, G.-X. Wang, R.S. Haque, L.M. Almara, New phase diagrams with anomalous region, supercritical solid-like state, liquid phase boundary, and dwij point, *J. Supercrit. Fluids*, 224, 2025.

[3] V. V. Brazhkin, Y. D. Fomin, A. G. Lyapin, V. N. Ryzhov, and K. Trachenko, Two liquid states of matter: A new dynamic line on a phase diagram, *Phys. Rev.* E, 85 (3), 2012.

[4] J.-Q. Guo, M.-J. Li, Y.-L. He, T. Jiang, T. Ma, J.-L. Xu, F. Cao, A systematic review of supercritical carbon dioxide(S-CO2) power cycle for energy industries: Technologies, key issues, and potential prospects, *Energy Conversion and Management*, 258, 2022.

[5] G. Liao, L. Liu, J. E, F. Zhang, J. Chen, Y. Deng, H. Zhu, Effects of technical progress on performance and application of supercritical carbon dioxide power cycle: A review, *Energy Conversion and Management*, 199, 2019.

[6] Moisseytsev, A., & Sienicki, J. J. (2007). Investigation of Alternative Layouts for the Supercritical Carbon Dioxide Brayton Cycle for Sodium-Cooled Fast Reactors. ANL-GenIV-103, Argonne National Laboratory.

[7] B. Thomson and I. Han, 2005: Ocean Storage, *Carbon Dioxide Capture and Storage: A Special Report of IPCC Working Group III*, Cambridge University Press, New York, 277-318.

[8] V.E. Onyebuchi, A. Kolios, D.P. Hanak, C. Biliyok, V. Manovic, A systematic review of key challenges of CO2 transport via pipelines, *Renewable and Sustainable Energy Reviews,* 81, Part 2, 2018.

[9] L.M. Almara, G. X. Wang, and V. Prasad, Conditions and thermophysical properties for transport of hydrocarbons and natural gas at high pressures: Dense phase and anomalous supercritical state, *J. Gas Sci. Eng*., 205072, 2023

[10] V. Prasad, L.M. Almara, and G.X. Wang, Ultra-long-distance transport of supercritical natural gas (SNG) at high-mass flow rates via pipelines through land, underground, water bodies, and ocean, *J. Gas Sci. Eng*., 205053, 2023.

ACKNOWLEDGEMENTS

This research has been supported by US National Science Foundation's Collaborative Research Awards #2327571 to the University of North Texas and #2327572 to The University of Akron.